

Figures



Figure 1. Application of the semi-supervised CRF at Seabright beach for generation of DCNN training tiles and ground-truth labeled images. From left to right, (A) the input image, (B) the hand-annotated sparse labels, and (C) the resulting CRF-predicted pixelwise labeled image.

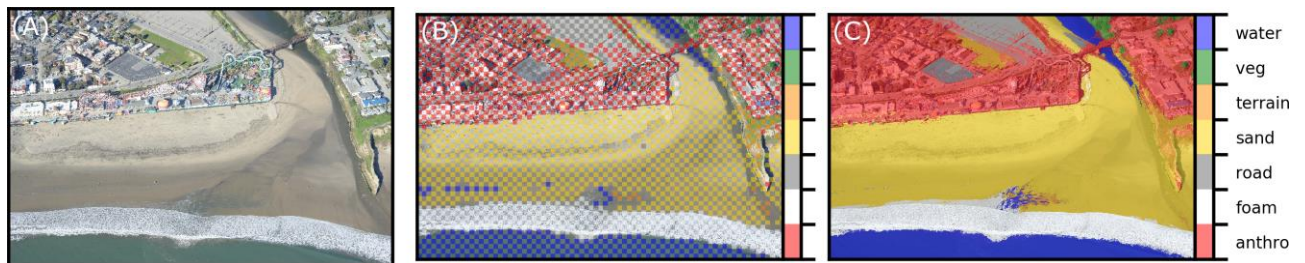


Figure 2. Application of the unsupervised CRF for pixelwise classification, based on unary potentials of regions of the image classified using a DCNN. Example comes from Seabright beach. From left to right, (A) the input image, (B) the DCNN-estimated sparse labels, and (C) the resulting CRF-predicted pixelwise labeled image.



Figure 3. Example tiles from NWPU data set. Classes, from left to right, are beach, chaparral, desert, forest, island, lake, meadow, mountain, river, sea ice, and wetland.



Figure 4. Example tiles from Seabright beach. Classes, from left to right, are anthropogenic/buildings, foam, road/pavement, sand, other natural terrain, and vegetation.



Figure 5. Example tiles from Lake Ontario shoreline. Classes, from left to right, are anthropogenic/buildings, sediment, other natural terrain, vegetation, and water.

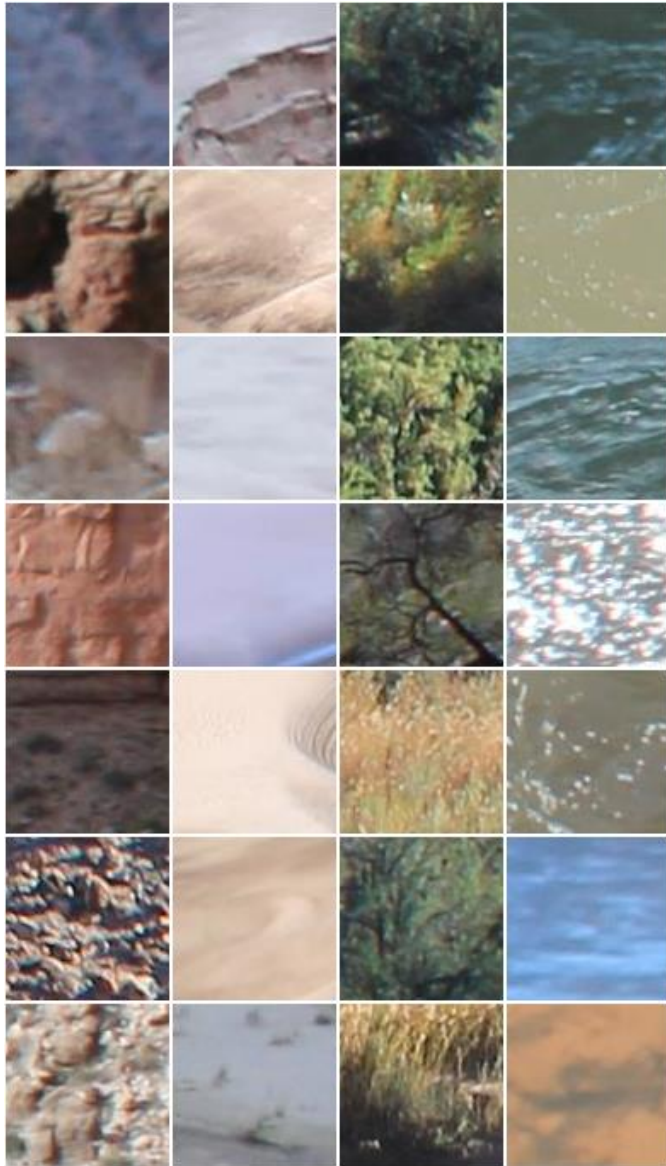


Figure 6. Example tiles from Grand Canyon. Classes, from left to right, are rock/scree, sand, vegetation, and water.

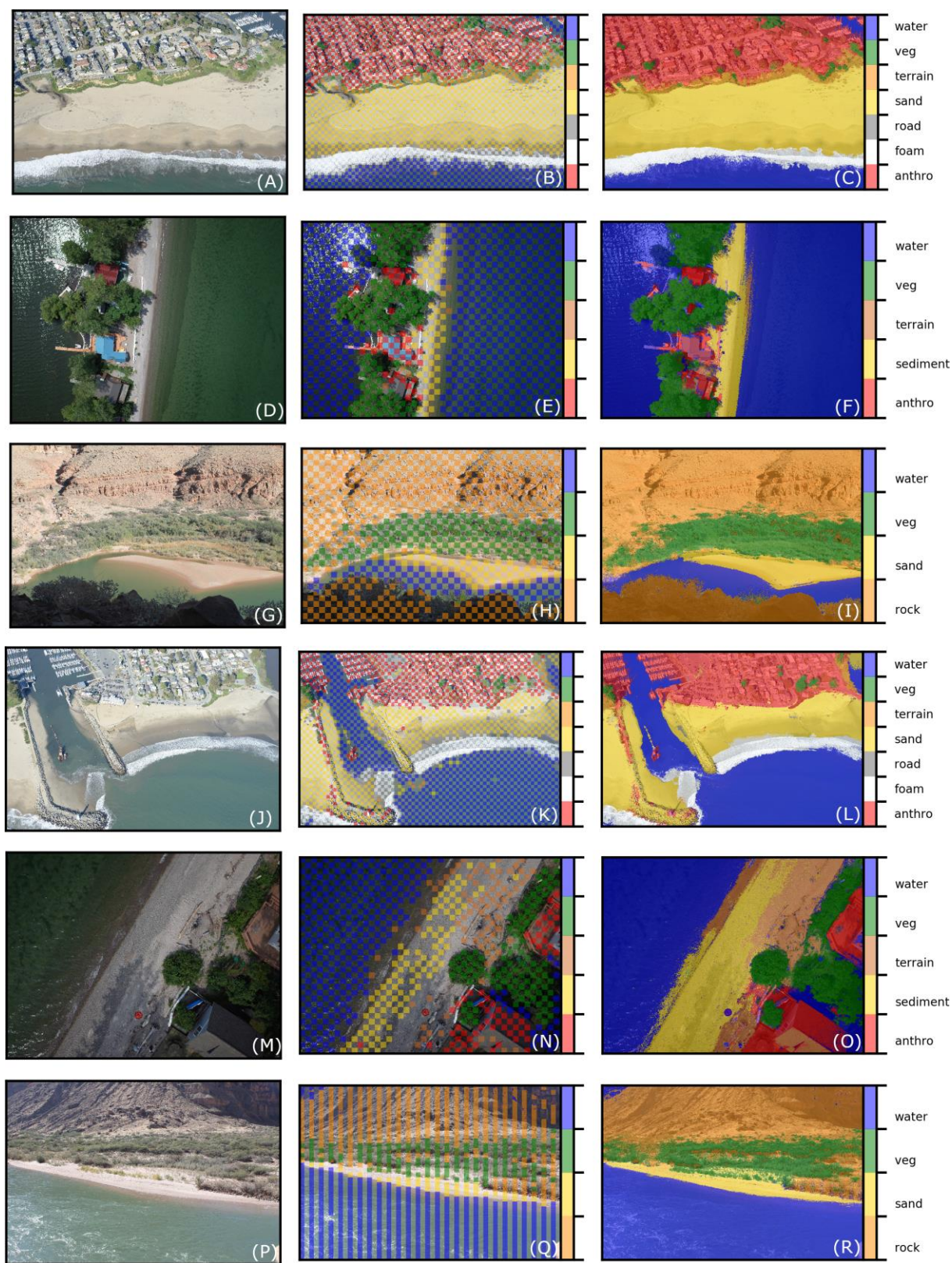


Figure 7. Example images (left column), DCNN-derived unary potentials (middle column), and CRF-derived pixelwise semantic segmentation (right column).

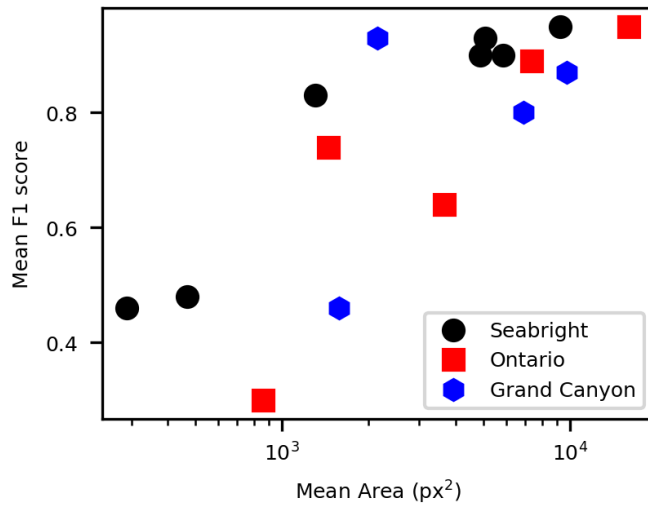


Figure 8. Average F1 score (harmonic mean of precision and recall) versus average area (in square pixels) of classes

Supplemental Figures

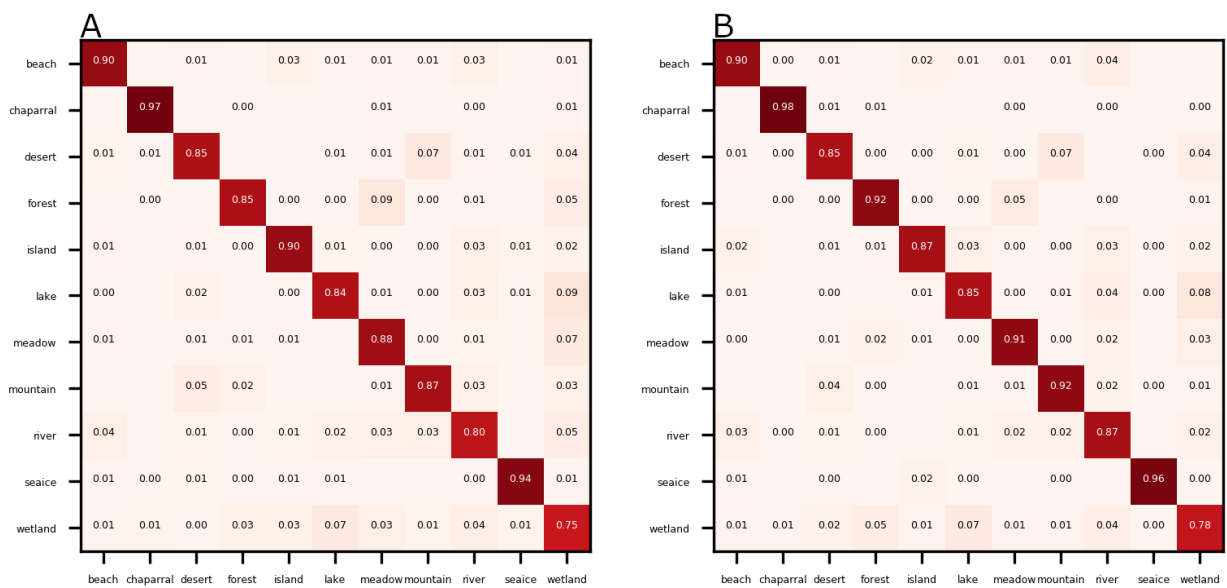


Figure S1. Matrices of correspondences (proportion correctly classified) between true (left axis) and DCNN-estimated (bottom axis) labels, based on tiles generated from NWPU imagery, on size 96 (A) and 224 (B) pixels.

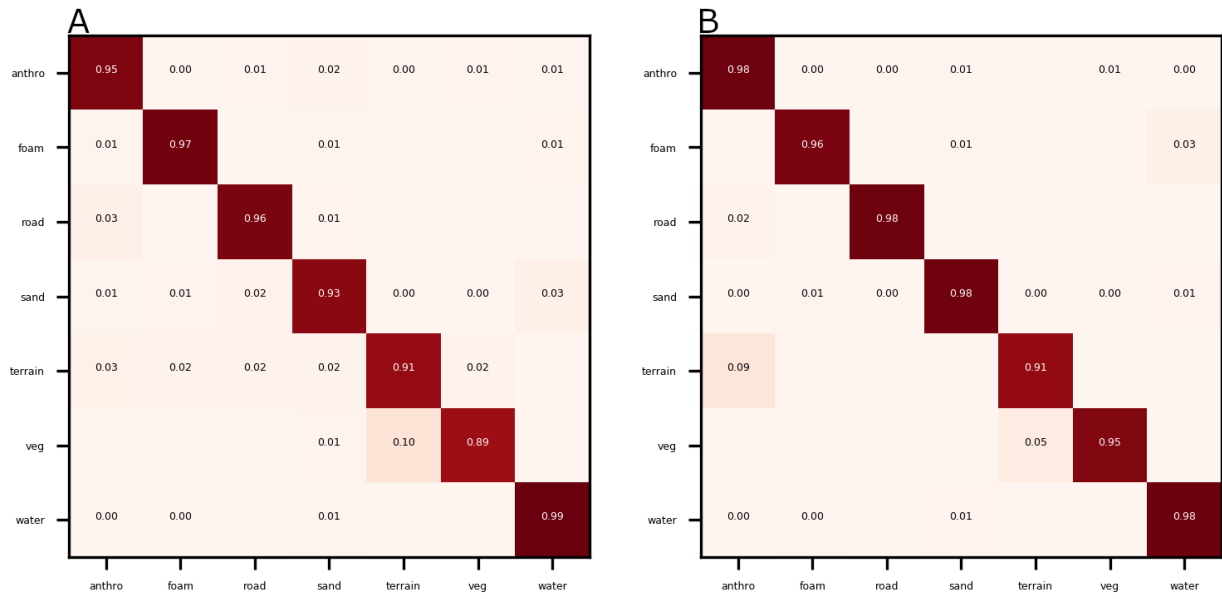


Figure S2. Matrices of correspondences (proportion correctly classified) between true (left axis) and DCNN-estimated (bottom axis) labels, based on tiles generated from imagery at Seabright beach, on size 96 (A) and 224 (B) pixels.

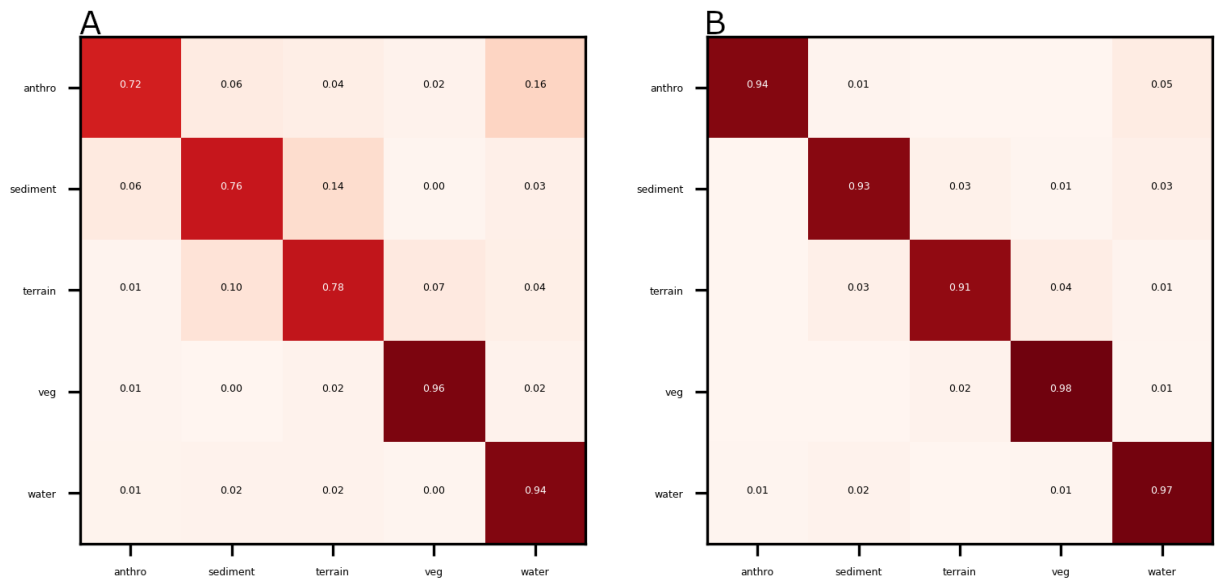


Figure S3. Matrices of correspondences (proportion correctly classified) between true (left axis) and DCNN-estimated (bottom axis) labels, based on tiles generated from imagery at Lake Ontario, on size 96 (A) and 224 (B) pixels.

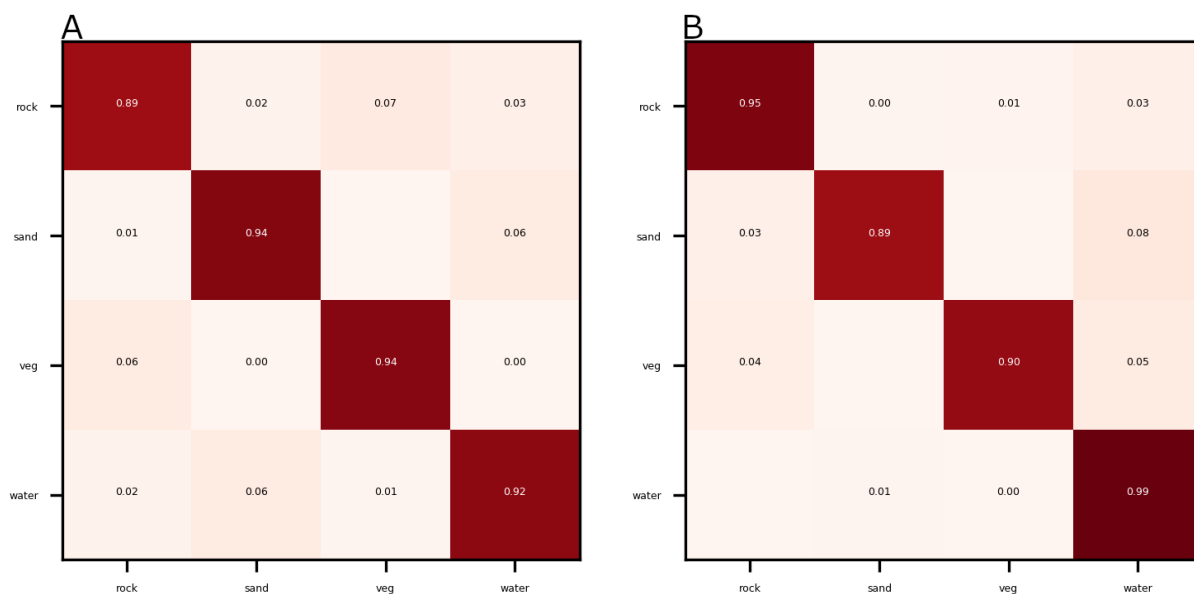


Figure S4. Matrices of correspondences (proportion correctly classified) between true (left axis) and DCNN-estimated (bottom axis) labels, based on tiles generated from imagery at Grand Canyon, on size 96 (A) and 224 (B) pixels.

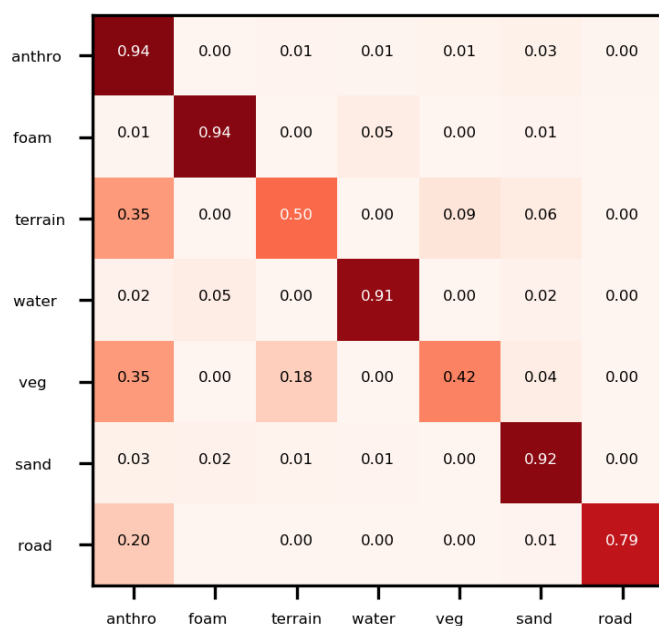


Figure S5. Matrix of correspondences (proportion correctly classified) between true (left axis) and DCNN-CRF-estimated (bottom axis) pixelwise labels, using test imagery at Seabright beach.

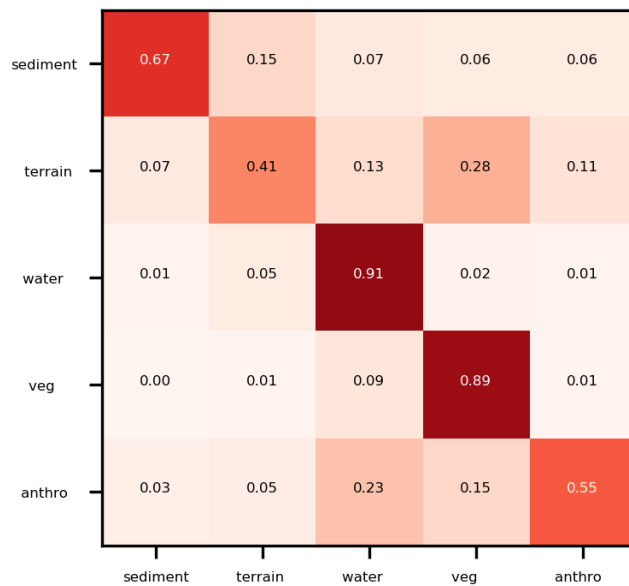


Figure S6. Matrix of correspondences (proportion correctly classified) between true (left axis) and DCNN-CRF-estimated (bottom axis) pixelwise labels, using test imagery at Lake Ontario.

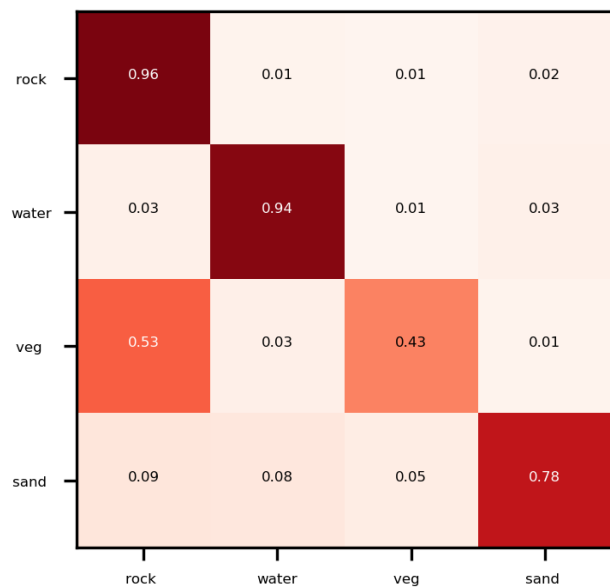


Figure S7. Matrix of correspondences (proportion correctly classified) between true (left axis) and DCNN-CRF-estimated (bottom axis) pixelwise labels, using test imagery at Grand Canyon.